Cancer Chemother Pharmacol (2007) 59:337–348
DOI 10.1007/s00280-006-0275-9

ORIGINAL ARTICLE

Irinotecan changes gene expression in the small intestine of the rat with breast cancer

Joanne M. Bowen · Rachel J. Gibson · Adrian G. Cummins · Anna Tyskin · Dorothy M. K. Keefe

Received: 16 February 2006 / Accepted: 20 May 2006 / Published online: 24 June 2006

Abstract
Purpose The aetiology of mucositis is complex involving change in gene expression, altered apoptosis and interaction between epithelial and subepithelial compartments. This is the first investigation using microarray to assess chemotherapy-induced changes in the gut. The aims of this study were to identify genes that are altered by irinotecan, to determine how these genes contribute to apoptosis and to identify any potential gene families and pathways that are important for mucositis development.
Methods Tumour-bearing female dark Agouti rats were administered twice with 150 mg/kg of irinotecan and killed 6 h after the final dose. Jejunal tissue was harvested and RNA was isolated. cDNA was synthesised and purified, prior to hybridisation and microarray analysis. A 5-K oligo clone set was used to investigate gene expression. Results from the microarray were quantified using RT-PCR.
Results Many genes were significantly up- or down-regulated by irinotecan. In particular, multiple genes implicated in the mitogen-activated protein kinase (MAPK) signalling pathway were differentially regulated following treatment. These included interleukin 1 receptor, caspases, protein kinase C and dual-specificity phosphatase 6. RT-PCR was used to confirm effects of irinotecan on caspase-1 expression in jejunal tissue and was significantly increased 6 h after treatment with irinotecan.
Conclusions This study has identified MAP kinase signalling as being involved with irinotecan-induced intestinal damage and confirms previous findings with radiation-induced oral mucosal damage, which also implicated this pathway. Microarrays are emerging as a valuable tool in mucositis research by linking such findings. The common pathway of chemotherapy- and radiotherapy-induced damage, which utilises the caspase-cascade, may be a useful target to prevent apoptosis following cancer treatment.

Keywords Microarray · Mucositis · Chemotherapy · Gastrointestinal tract

J. M. Bowen (✉) · R. J. Gibson · D. M. K. Keefe
Department of Medical Oncology, Royal Adelaide Hospital, North Terrace, Adelaide 5000, South Australia, Australia
e-mail: joanne.bowen@adelaide.edu.au

J. M. Bowen · R. J. Gibson · A. G. Cummins · D. M. K. Keefe
Department of Medicine, University of Adelaide, Adelaide, South Australia, Australia

A. G. Cummins
Department of Gastroenterology and Hepatology, The Queen Elizabeth Hospital, Woodville South, South Australia, Australia

A. Tyskin
Hanson Institute, Adelaide, South Australia, Australia

A. Tyskin
Department of Mathematics, University of Adelaide, Adelaide, South Australia, Australia

Introduction

Gastrointestinal mucositis is a major oncological problem caused by the cytotoxic effects of cancer chemotherapy. The condition affects the entire gastrointestinal tract and causes pain and ulceration in the mouth and small and large intestines. In addition it causes abdominal bloating, vomiting and diarrhoea [22, 36]. Recent

research has indicated that biological mechanisms underlying mucositis are the result of a number of dynamic and interactive molecular and cellular events that occur in all layers of the mucosa [42–45]. Briefly, the initiating events of cytotoxic agents are the generation of oxidative stress and reactive oxygen species which both cause damage to all the tissue components of the mucosa. Second, the transcription factor NF-κB is activated and leads to the up-regulation of many genes, including those responsible for the production of the pro-inflammatory cytokines, as well as adhesion molecules and cyclooxygenase-2. This results in further tissue injury and apoptosis. During the third phase, a feedback loop occurs whereby tumour necrosis factor (TNF) acts on a number of pathways to reinforce NF-κB activation and the ceramide pathway. Following this, an ulcerative phase is observed with bacterial colonisation, subsequent increased pro-inflammatory cytokine production and hence inflammation. Finally, healing occurs with renewal of epithelial proliferation and differentiation, and re-establishment of the normal local microbial flora.

Irinotecan hydrochloride (CPT-11) is a new chemotherapy drug used primarily to treat advanced colon cancer. It belongs to the topoisomerase I interactive class of anti-cancer drugs, targeting the DNA-topoisomerase I complex and arresting replication leading to cell death [51]. Irinotecan is highly toxic to both the small and large intestines, causing extensive crypt damage with accompanying change in mucin distribution [12, 17]. The use of irinotecan in the clinic often results in adverse side effects with dose-limiting toxicity including severe diarrhoea and leukopenia [1].

Irinotecan causes two types of diarrhoea. First, an early onset secretory diarrhoea which is cholinergic in nature (this can be ameliorated by the co-administration of atropine during treatment), and second, a delayed onset diarrhoea which is prolonged and can be life-threatening. The exact nature of this delayed-onset diarrhoea has yet to be fully elucidated, although possible explanations include alteration in normal intestinal microflora and subsequent change in β-glucoronidase activity, changes in mucin composition and also development of enterocolitis with accompanying altered water and electrolyte secretion [9, 12, 47].

Although the exact cause of downstream side effects of irinotecan, such as diarrhoea, is still unknown, strong evidence exists for the additional role of apoptosis in mediating damage in the intestines. Previous studies have documented an increase in apoptosis within crypts that peaks by 24 h following administration of the cytotoxic. This is followed by a period of crypt hypoplasia that precedes loss of epithelial morphology [5, 12, 13].

Caspases play a central role in the regulation and execution of apoptotic cell death and are likely to be important in irinotecan-induced intestinal damage. Specific caspases are activated in response to varying death-inducing signals. The initiator caspases-8 and -10 are recruited following ligation of cell membrane death receptors, while caspase-9 responds to cytochrome c release from the mitochondria, and caspase-12 is activated in response to endoplasmic reticulum stress [27, 35]. Caspases-1 and -5 are activated when complexed with the recruiter protein NALP1 or adaptor protein Ipaf as part of the inflammasome [31].

Genome-wide analysis through microarray technology can provide a powerful tool to investigate changes in gene expression occurring in multiple tissue layers simultaneously. Thus the primary aim of this study was to identify the genes that are up- and down-regulated by irinotecan treatment in the rat small intestine. Secondary aims were to: (1) determine how these gene changes contribute to apoptosis and (2) identify any potential candidate genes that are important for mucositis development. An understanding of the genetic pathways utilised by irinotecan to induce intestinal damage would allow for improved intervention therapies to be designed.

Materials and methods

Laboratory animals

This study was approved by the Animal Ethics Committees of the Institute of Medical and Veterinary Sciences, Adelaide and of the University of Adelaide and complied with National Health and Research Council (Australia) Code of Practice for Animal Care in Research and Training (2004). Female dark Agouti (DA) rats, aged 6–8 weeks and weighing approximately 160 g were purchased from the Institute of Medical and Veterinary Sciences MedVet division, group-housed and kept under a 12-h light/dark cycle with free access to food and water until the study commenced (approximately 2 weeks). All animals used in this study were tumour-bearing. The mammary adenocarcinoma model has been used by our group for a number of years and has been described elsewhere [13–15].

Experimental design

This study was divided into two parts—microarray and real-time PCR experiments

Microarray experiment

Eight female DA rats were implanted with tumour inoculum of 4.0×10^6 cells in 0.2 ml of phosphate-buffer saline (PBS) subcutaneously (s.c.) into each flank and randomly divided into two groups ($n = 4$). Tumours were allowed to grow for 9 days after which, group 1 rats were administered irinotecan (150 mg/kg intraperitonally) on two consecutive days to induce gastrointestinal mucositis. This dose induces reproducible gastrointestinal mucositis [12, 13]. Irinotecan was administered in a sorbitol/lactic acid buffer (45 mg/ml sorbitol/0.9 mg/ml lactic acid) required for activation of the drug. Group 2 rats received buffer only and were designated controls. All rats also received 0.01 mg/kg s.c. atropine immediately prior to irinotecan to reduce any cholinergic reaction to the treatment. Animals were culled by CO_2 asphyxiation and cervical dislocation 6 h after the second injection of irinotecan. The gastrointestinal tract (GIT) from the pyloric sphincter to the rectum was removed and flushed with sterile, chilled 0.9% w/v saline. Two-centimetre samples of small intestine (jejunum) at 25% of the length of the small intestine from the pylorus were collected, snap frozen in liquid nitrogen and stored at –70°.

RNA extraction and cDNA synthesis Total RNA was isolated from 30 mg of homogenised whole jejunal tissue using TRIzol® reagent (Invitrogen Life Technologies, Mulgrave, VIC). This was performed according to the manufacturer's instructions.

To 20 μg of RNA the following were added: 3 μg of polyA and 3 μg of hexamers. This was incubated for 10 min at 70°C to denature RNA. The denaturation was halted by placing samples on ice. Reverse transcription was carried out by adding 6 μl of M-MLV buffer, 0.6 μl dNTPs (500 μM), 2 μl of M-MLV reverse transcriptase (200 U/μl, Invitrogen) and samples were incubated for 150 min at 42°C. Any remaining RNA was degraded by adding 10 μl of sodium hydroxide (0.25 M) and 10 μl of EDTA (0.5 M) and samples were incubated for 15 min at 65°C. The reaction was neutralised by adding 15 μl of 0.2 M acetic acid.

cDNA purification and dye coupling The QIAquick PCR purification kit (QIAGEN) was used to purify cDNA according to the manufacturer's instructions from 20 μg of RNA. cDNA was added to Cy 3/5 tubes (Amersham, Buckinghamshire, UK) and incubated in the dark for 60 min at room temperature. Samples were re-purified through QIAGEN columns; however this time, cDNA from one control and one experimental rat (which were coupled with different dyes) were each placed on one column together for a final total of four mixed samples. The mixed samples were eluted with 90 μl of sterile Milli-Q water. The cDNA was pelleted and dried in a speedvac for 30 min at 50°C. A blocking step was carried out by adding 0.64 μl of yeast tRNA, 4 μl of PolyA (2 mg/ml; Sigma, St Louis, MO, USA) and 20 μl of Cot-1 DNA (1 mg/ml; Invitrogen) to the cDNA. Re-drying occurred in a speedvac and the resultant pellet was dissolved in 16 μl of formamide and 16 μl of 6.25 × SSC (1 M of sodium citrate, 1 M of sodium chloride). The samples were heated for 4 min at 100°C before being placed on ice to halt reaction. Finally, samples were spun quickly and 0.2 μl of 10% sodium dodecyl sulphate (SDS) was added.

Hybridisation and slide analysis Four rat 5-K MWG oligo array glass slides were purchased from the Clive and Vera Rammaciotti Centre for gene function analysis (University of NSW, Sydney, NSW). To prepare the slides, they were baked for 30 min at 60°C before being washed in 0.1% SDS for 1 min at 95°C. They were quickly rinsed in 5% ethanol, followed by 0.2 × SSC. Slides were dried by centrifugation. Hybridisation chambers were cleaned and chamber reservoirs were filled with 1 × SSC to keep slides humid. A 30-μl sample of cDNA was used for each microarray slide. Slides were placed into chambers and incubated overnight at 42°C. Slides were washed in 0.5 × SSC, followed by 0.2 × SSC for 5 min each and then dried by centrifugation. The microarray slides were scanned using a GenePix 4000B Scanner driven by GenePix Pro 4.0 (Axon Instruments, Foster City, CA, USA). All analyses were performed using the freely available statistical programming and graphics environment R (http://www.cran.r-project.org) [50]. The "SPOT" software package (http://www.experimental.act.cmis.csiro.au/Spot/index.php) was used to identify spots by adaptive segmentation method and subtract backgrounds utilising morphological opening approach. The extracted information was analysed using the limma package (http://www.bioinf.wehi.edu.au/limma). All data were normalised to remove from the expression measures any systematic trends which arise from the microarray technology rather than from differences between the probes or between the target RNA samples hybridised to the arrays. This was done by the Loess print tip method which corrects for dye bias and intensity within each group of adjacent spots printed by one pin (print tip). Differentially expressed genes were ranked on Bayesian posterior log odds calculated with limma [28]. The empirical Bayes method was used to shrink the gene-wise sample variances towards common values

and, in so doing, augmenting the degrees of freedom for the individual variances. This approach combines expression ratios and their variability between replicates to rank the genes [29].

Real-time PCR experiment

Archival frozen tissue from 24 tumour-implanted DA rats that were treated identically to that described earlier were used to investigate mRNA expression following chemotherapy in the small intestine [6]. Resected samples were taken from 6-, 24- and 48-h time points and untreated control rats ($n = 6$) [6]. Quantification of changes in expression of genes of interest was performed by a DNA Engine OPTICON 2 Continuous Fluorescence Detector (MJ Research, Bio-Rad). PCR primers for rat 18S ribosomal RNA (Genbank # X01117) were designed according to published information [2], while primers for rat caspase-1 (Genbank # U14647) were designed by Primer Premier version 5 (PREMIER Biosoft International, Polo Alto, CA, USA).

18S forward 5′-GGGAGGTAGTGACGAAAAA TAACAA
18S reverse 5′-TTGCCCTCCAATGGATCCT
Caspase-1 forward 5′-CACTAAAAAAGGACCCC
Caspase-1 reverse 5′-ATGGACCTGACTGAAGC

Primer pairs were specific for a 101- and 98-base pair product, respectively. 18S and caspase-1 oligonucleotide standards were synthesised by Geneworks (Adelaide, South Australia, Australia) and corresponded to their respective primer pair product. In each experiment, duplicates of 18S and caspase-1 oligonucleotide standards were added in a dilution series along with unknown samples. These were amplified in a 20-µl reaction containing 2× DyNAmo™ SYBR® Green qPCR master mix (Finnzymes, Keilaranda, Espoo, Finland) and 1 µl of cDNA template. The real-time thermal PCR profile consisted of one cycle of 95°C for 7 min, 40 cycles of 95°C for 15 s and 60°C for 1 min and one cycle of 72°C for 10 min. Fluorescence measurements were recorded at 60°C each cycle. The cycle threshold value (CT) was used to assess the quantity of 18S and caspase-1 gene expression. The CT was fixed manually in each experiment at the exponential phase of the PCR. The relative copy number of each transcript was determined by interpolating the CT values of the unknown sample to each standard curve and the obtained values were normalised to the 18S copy number. The lack of primer dimer, non-specific product accumulation or DNA contamination was assessed by melt curve analysis. Dissociation curves showed a single peak corresponding to a melting temperature of 76.2 ± 0.2 for 18S and 77.8 ± 0.3 for caspase-1.

Statistics

The extracted microarray information was analysed using the limma package (http://www.bioinf.wehi.edu.au/limma). Differentially expressed genes were ranked on moderated *t*-statistics [41] and those with absolute values of *t* above 5 were followed up further. As there is no consensus on appropriate adjustment of *P* values in the context of microarrays, the cut-off level was chosen on a combination of statistical and biological indicators. The real-time PCR results were analysed by one-way ANOVA and Tukeys post-hoc test, with a P value < 0.05 considered significant.

Results

Microarray experiment

The investigation into gene expression profiles in control and irinotecan-treated rats by microarray analysis revealed many gene differences between the two groups. The data was analysed to create a shorter list of genes according to reproducibility and log ratio data. This resulted in up- and down-regulated genes (Table 1). Genes with similar cellular roles were grouped accordingly into categories using the ontology resource EGAD (The Expressed Gene Anatomy Database, www.tigr.org/tdb/egad) (Table 2). The most highly represented genes thought to be important in mucositis development were associated with chromosome structure (5), cell cycle regulation (4), apoptosis (5), immunological responses (7) and protein turnover (15). These are involved in a number of biological pathways, and importantly, genes that are associated with the MAP kinase stress pathway were identified which included interleukin 1 receptor antagonist, caspases, protein kinase C and protein tyrosine phosphatases. A literature search was conducted through web-based resource, PubMed (Entrez, National Centre for Biotechnology Research) to identify from this study, up-regulated genes implicated in development of intestinal mucositis. This search identified caspases and dihydropyrimidine dehydrogenase (DPD) as genes closely associated with intestinal damage in response to chemotherapy treatment. The well-defined role of caspases in the apoptotic pathway led to the choice of caspase-1 for further investigations by real-time PCR.

Table 1 List of genes that had altered expression following treatment with irinotecan. Genes above the line were those found to be upregulated. Genes below the line were found to be down regulated

Rank	GenBank	*t*	Ratio	Name
5	X59961	11.458	2.538	Genes for H2A and H2B histones
8	U35775	10.308	1.866	Adducin 3 (gamma)
20	X15741	8.6564	2.971	Polymeric immunoglobulin receptor
21	M31229	8.6127	1.859	Histone H1d gene
22	K01934	8.5298	2.364	Hepatic product spot 14
24	U14647	8.3558	2.566	Caspase 1
26	AF149250	8.2494	2.315	Potassium intermediate/small conductance calcium activated channel, subfamily N member 4
27	M28409	7.9916	1.904	Testis-specific histone H1t and histone H4t
29	X13554	7.8979	1.871	H4 somatic histone
33	L35317	7.5361	1.974	Isocitrate dehydrogenase 1 (NADP+)
39	M99567	7.1696	1.588	Phospholipase C beta 3
41	M12335	7.0227	2.029	Nucleus-encoded mitochondiral carbamyl phosphate synthetase 1 gene exon 13 precusor
42	AF091565	6.9837	1.667	Olfactory receptor 837
43	JO3588	6.9697	1.675	Guanidinoacetate methyltransferase
44	U59462	6.9603	1.719	Lectin, galactose binding soluble 9
45	S68245	6.9148	1.534	Carbonic anhydrase IV
46	S87522	6.9099	1.748	Leukotriene A4 hydrolase
53	U49062	6.6521	1.849	CD24 antigen
55	L19706	6.5871	1.754	H3 histone gene putative
57	M58040	6.499	1.987	Transferrin receptor
58	JO2954	6.4976	1.928	Calbidin 3 (vitamin D-dependent calcium-binding protein)
60	U73174	6.4246	1.664	Glutathione reductase
62	D38067	6.3851	1.792	DNA for UDP glucuronosyltransferase
64	L23077	6.3266	1.486	Zinc finger protein
70	KO3249	6.1279	1.676	Enoyl-coenzyme A hydratase/3-hydroxyacyl coenzyme A dehydrogenase
71	U57042	6.0045	1.728	Adenosine kinase
73	D10757	5.9984	1.464	Proteasome subunit R-RING12
83	XO7286	5.7377	1.5	Protein kinase C alpha
84	D85035	5.7318	1.73	Dihydropyrimidine dehydrogenase
85	D10729	5.7159	1.624	Proteasome subunit RC1
86	ABO37424	5.708	1.433	Aldo-keto reductase family 7
87	U34685	5.6303	1.739	Caspase 3
92	AF170918	5.5261	1.455	Aldehyde dehydrogenase family 9 subfamily A1
101	U50194	5.2553	1.477	Tripeptidyl peptidase II
107	M73714	5.188	1.439	Aldehyde dehydrogenase family 3 subfamily A2
109	M27466	5.1403	1.444	Cytochrome c oxidase subunit Vlc
110	U66322	5.1347	1.732	Leukotriene B4 12-hydroxydehydrogenase
112	X56917	5.1097	1.525	Inositol 1,4,5-triphosphate 3-kinase A
115	D87515	5.0585	1.390	Arginyl aminopeptidase
117	U75391	5.0494	1.531	B-cell receptor-associated protein 37 (BAP-37)
120	AF120100	5.0142	1.407	Thiopurine methyltransferase
121	U57501	5.0033	1.48	Protein tyrosine phosphatase receptor type G
1	JO3026	−21.899	0.153	Matrix Gla protein
2	AF157026	−15.025	0.364	Solute carrier family 34 (sodium phosphate) member 2
3	X61381	−13.544	0.217	*Rattus rattus* interferon induced
4	L29512	−12.194	0.128	Tissue inhibitor of metalloproteinase 1
6	M65253	−10.739	0.352	Matrix metallopeptidase 10
10	AF164039	−9.8673	0.261	Interferon-inducible protein variant 10
11	M11794	−9.7998	0.151	Metallothinein-2 and metallothinein-1 genes; metallothionein 1
12	U17035	−9.6032	0.325	(mob-1)
14	AF164040	−9.1193	0.381	Interferon-induced transmembrane protein 2 (1-8D)
15	AF159104	−9.0425	0.436	CD63 antigen
17	U86635	−8.7368	0.541	Glutathione *S*-transferase,mu 5
18	U27767	−8.7239	0.557	Regulator of G-protein signalling 4

Table 1 continued

23	X12554	−8.4818	0.515	Cytochrome c oxidase, subunit Vla polypeptide 2
25	AF241259	−8.3498	0.6	Regulator of G-protein signalling 5
28	AJ132717	−7.9482	0.576	S100 calcium-binding protein A6 (calcyclin)
30	S85184	−7.8369	0.471	Cyclic protein-2 (CP-2) partial cs; cathepsin L pro-enzyme
31	M28259	−7.7967	0.558	Fibronectin gene exons 2b and 3a
32	D88666	−7.7012	0.518	Phosphatidylserine-specific phospholipase A1
34	M30692	−7.4122	0.274	Ly6-A antigen gene, exon 2 putative
35	D38629	−7.3849	0.545	Adenomatosis polyposis coli
36	D88250	−7.3021	0.564	Complement component 1 s subcomponent
37	AF223677	−7.2419	0.615	Steroid sensitive gene 1
38	JO3753	−7.2256	0.525	ATPase Ca++ transporting, plasma membrane 1
40	AF220102	−7.0251	0.581	Interleukin enhancer binding factor 3
47	Af132045	−6.9039	0.545	Foocen-m2 alternate splice product
48	D16308	−6.889	0.559	Cyclin D2
49	X71127	−6.7862	0.587	Complement component 1q subcomponent beta polypeptide
50	X61667	−6.7232	0.518	Ant1 adenine nucleotide translocator
51	U48255	−6.7215	0.356	CD59 antigen
52	AF257237	−6.7066	0.191	Oxytocin receptor
54	M14972	−6.6293	0.598	Cytochrome P-450-LA-omega
56	AF196201	−6.5488	0.594	Similar to T cell receptor V delta 2
61	AF136583	−6.3987	0.523	Polo-like kinase 2 (Drosophila)
63	U31598	−6.3588	0.558	Major histocompatibility complex class II DMA alpha
65	X70871	−6.2858	0.426	Cyclin G1
66	X62952	−6.2114	0.555	Vimentin
67	D00753	−6.1591	0.239	Serine protease inhibitor
68	AB032766	−6.1472	0.602	Legumain
69	U25055	−6.1304	0.493	Solute carrier family 28 member 2
72	Y10019	−5.9994	0.387	Gremlin 1 homolog, cystein knot superfamily(xenopus laevis)
74	AF131912	−5.9704	0.608	Ephrin A2
75	AF165887	−5.9677	0.691	Branched chain aminotransferase 1, cytosolic
76	AF023302	−5.8828	0.564	Flotillin 2
77	S76513	−5.8472	0.53	Bcl-*x*=apoptosis inhibitor
78	M62781	−5.8357	0.517	Insulin-like growth factor binding protein 5
79	X56747	−5.821	0.686	Fetal intestinal lactase-phlorizin hydrolase precursor, partial
80	AF20901	−5.8021	0.637	Interferon gamma receptor 1
81	D10607	−5.7777	0.645	Cystatin beta
82	M29853	−5.7598	0.476	Cytochrome P450 family 4, subfamily b, polypeptide 1
88	S61804	−5.5975	0.587	*O*6-methylguanine-DNA methyltransferase
89	AF144756	−5.5816	0.530	Fatty acid binding protein 4 adipocyte
91	S57478	−5.5665	0.622	Lipocortin I
93	AB043636	−5.501	0.475	Potassium inwardly-rectifying channel subfamily J member 8
94	AF184983	−5.4806	0.667	Glycoprotein (transmembrane) nmb
95	U42627	−5.4354	0.635	Dual-specificity phosphatase 6
96	U06752	−5.4346	0.50	Similar to heterodimeric complex composed of a mucin subunit ASGP-1
97	X13252	−5.4334	0.612	Cholinergic receptor, nicotinic, epsilon polypeptide
98	AF205713	−5.3837	0.587	Glial cell line derived neurotrophic factor
99	AF070475	−5.360	0.65	Solute carrier family4, sodium bicarbonate co-transporter member 7
100	AF087037	−5.2709	0.618	B-cell translocation gene 3
102	AF136230	−5.2531	0.580	Bcl2-like 1
103	AF159097	−5.2332	0.626	Seminal vesicle secretion 5
104	K02246	−5.2291	0.173	Cytochrome P450c (methylcholanthrene-inducible) gene
105	L04739	−5.2158	0.638	Plasma membrane calcium ATPase isoform 1 gene, partial cds; isoform 1
106	AJ409332	−5.2004	0.654	Tissue inhibitor of metalloproteinase 2
108	J04791	−5.1772	0.696	Ornithine decarboxylase 1
111	AF153193	−5.1273	0.676	Winged helix/forkhead transcription factor HFH1 gene
113	L07316	−5.0922	0.706	Dipeptidase 1 (renal)
114	M84719	−5.0864	0.719	Flavin-containing monooxygenase 1
116	L29191	−5.0546	0.619	Fibronectin (cell-, heparin- and fibrin-binding domains) gene encoding three fibronectin mRNAs
118	AB010119	−5.0464	0.678	T-complex testis expressed 1
119	Af111160	−5.0361	0.657	Glutathione *S*-transferase A5

Table 2 List of differentially regulated genes grouped according to functional classification

Cellular role	Gene	Regulation
Cell signaling/communication		
Cell adhesion/surface antigen	Fibronectin	Down
	CD24	Up
	Lectin, galactose binding	Up
	CD59	Down
	Ly6-A-antigen	Down
	CD63	Down
Channels/transport proteins	Ca++-activated K+ channel	Up
	ATPase	Down
	Potassium inwardly rectifying channel	Down
	Ant1	Down
	Solute Carrier family 4	Down
	Solute Carrier family 34	Down
	Solute Carrier family 28	Down
Effectors/modulators	Calcyclin	Down
	Vitamin D-dependent Ca++ binding protein	Up
	Dual specificity phosphate 6	Down
	Inositol 1,4,5 triphosphate	Up
	Polo-like kinase 2	Down
	Phospholipase C	Up
	Ephrin A2	Down
	Protein kinase C	Up
	Protein tyrosine phosphatase	Up
	Regulator of G-protein signaling 4	Down
Growth factors	Insulin-like growth factor binding protein 5	Down
	Glial cell line derived neurotrophic factor	Down
Receptors	Cholinergic receptor	Down
	Oxytocin receptor	Down
	Olfactory receptor 837	Up
	Interferon gamma receptor 1	Down
	Transferrin receptor	Up
	Polymeric Ig receptor	Up
Cell defence		
Immunology	Complement components 1q and 1s	Down
	Interluekin 1 receptor antagonist	Down
	Leukotriene B4 12-hydroxydehydrogenase	Up
	B-cell receptor associated protein 37	Up
	Major histocompatibility complex (MHC) class II-like alpha chain	Down
Apoptosis	*Caspase-1*	Up
	Caspase-3	Up
	Bcl-2 like 1	Down
	Bcl-xL	Down
Stress response	Heat shock protein 27	Down
	Ornithine decarboxylase 1	Down
Homeostasis	Metallothionein	Down
Cell division		
Cell cycle	Cyclin G	Down
	DRM protein	Down
	Cyclin D2	Down
	Adenomatosis polyposis coli	Down
Transcription	Zinc Finger Protein	Up
	Winged helix/forkhead transcription factor HFH1	Down
Chromosome structure	H2A and H2B histone	Up
	H3 histone	Up
	H4 somatic histone	Up
	H1d	Up
	H1t and H4t protein	Up

Table 2 continued

Cellular role	Gene	Regulation
Metabolism		
Amino acid	Carbamyl phosphate synthetase	Up
	Glutathione reductase	Up
	Nucleus-encoded mitochondrial carbamyl phosphate	Down
	Arginyl aminopeptidase	Up
	Glutathione *S*-transferase	Down
Lipid	Fatty acid-binding protein	Down
	Lipocortin	Down
	Aldehyde dehydrogenase families 3 and 9	Up
	Enoyl-coenzyme A	Up
	Phosphatidylserine-specific phospholipase	Down
Energy	Isocitrate dehydrogenase	Up
	Guanidinoacetate methyltransferase	Down
	Carbonic anhydrase IV	Up
	Cytochrome c oxidase Vlc	Up
	Cytochrome c oxidase Vla	Down
Drug	Dihydropyrimidine dehydrogenase	Up
	DNA for UDP glucuoronosyltransferase	Up
	Thiopurine methyltransferase	Up
	Cytochrome P450 isoenzyme	Down
Nucleotide	Adenosine kinase	Up
Carbohydrate	Aldo–keto reductase	Up
	Foetal intestinal lactase-phlorizin hydrolase precursor	Down
Xenobiotic	Flavin containing monooxygenase 1	Down
	Leukotriene A4 hydrolase	Up
Gene/protein expression		
Protein turnover	Cyclic protein-2	Down
	TIMP-1	Down
	TIMP-2	Down
	Cpi-26	Down
	Serine protease inhibitor	Down
	Legumain	Down
	Proteosome subunit RC	Up
	Branched chain aminotransferase 1	Down
	Matrix metallopeptidase 10	Down
	Cystatin beta	Down
	Proteosome subunit R-RING12	Up
	Transformation-associated protein	Down
	Dipeptidase 1	Down
	Tripeptidyl peptidase II	Up
	WDNM1	Down
Cell structure		
Extracellular matrix	Gamma adducin	Up
	Matrix Gla protein	Down
	Seminal vesicle secretion 5	Down
	Gremlin 1	Down
	Vimentin	Down
	Similar to heterodimeric complex	Down
	T-complex testis	Down
Unclassified	Hepatic product spot 14	Up
	Steroid sensitive gene 1	Down
	Foocen-m2	Down
	Flotillin 2	Down
	Thiopurine methyltransferase	Up
	Interleukin enhancer binding factor 3	Down
	Interferon-induced transmembrane protein 2	Down

Real-time PCR experiment

The histological results of this experiment are described elsewhere [13]. All treated rats experienced signs of mucositis, including weight loss and diarrhoea as well as morphological alterations [14, 15, 32]. Examples of irinotecan-induced changes in the small intestine are shown in Fig. 1. At 6 h, crypt apoptosis was the

hallmark feature of damage in the intestine, while at later time points there was evidence of lamina propria oedema and enterocyte attenuation. By 48 h, crypt hyperplasia and villous atrophy was also evident (Fig. 1).

One candidate up-regulated gene, caspase-1, was selected for further analysis by real-time PCR. Expression of caspase-1 mRNA in the rat jejunum was investigated in untreated controls and at 6, 24 and 48 h following irinotecan treatment (Fig. 2). There was a significant increase in caspase-1 expression from control levels at 6 h ($P < 0.05$). Expression returned to pre-treatment levels at 24 h and then modestly increased again at 48 h (Fig. 2). All samples were run with internal control rat rRNA 18S to allow for quantification. The expression of 18S did not change at any time point, as expected with an internal housekeeping gene (data not shown).

Discussion

This study investigated gene changes that occur in the rat small intestine following irinotecan treatment through simultaneous genome-wide analysis, and characterised the profile of expression of the apoptosis regulator, caspase-1. To the best of our knowledge this is the first investigation to use microarrays to assess chemotherapy-induced changes in the gut. We found multiple genes were significantly up-regulated and substantially more were significantly down-regulated. Particular interest was generated by the effect of irinotecan on multiple genes involved in the MAPK signalling pathway. Genes identified by microarray analysis that were differentially regulated following treatment included interleukin 1 receptor antagonist, caspases, protein kinase C and dual-specificity phosphatase 6. This finding not only implicates MAP kinase signalling with irinotecan-induced intestinal damage but also confirms previous research with radiation-induced oral mucosal damage also implicating this pathway [46]. Furthermore, the present study also confirms that the development of mucositis follows a common pathway [21, 23, 45].

The present study found that caspases-1 and -3 were up-regulated. The involvement of caspase-3 in apoptosis has been described in detail [16, 30, 35] and has

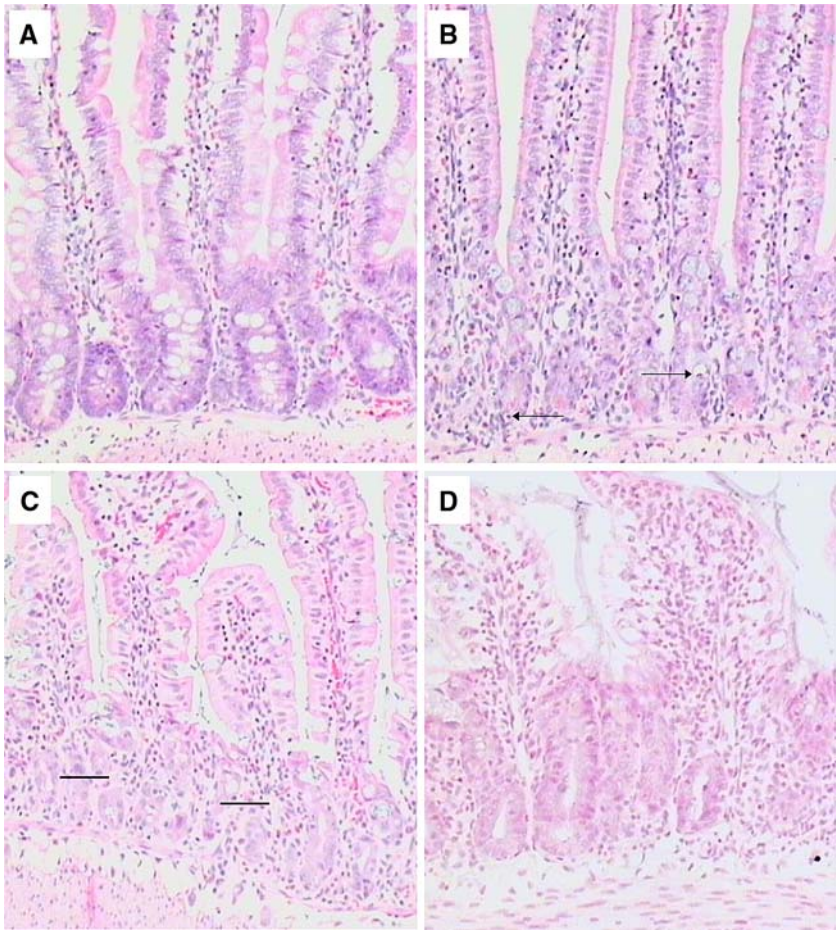

Fig. 1 Photomicrographs of rat jejunum stained with haematoxylin and eosin. **a** Untreated control, **b** 6 h, **c** 24 h and **d** 48 h. Irinotecan treatment caused changes in morphometry which included apoptosis (*arrows*) and crypt degeneration (*bars*) at early time points. Crypt hyperplasia and villous atrophy occurred at 48 h. Original magnification ×100

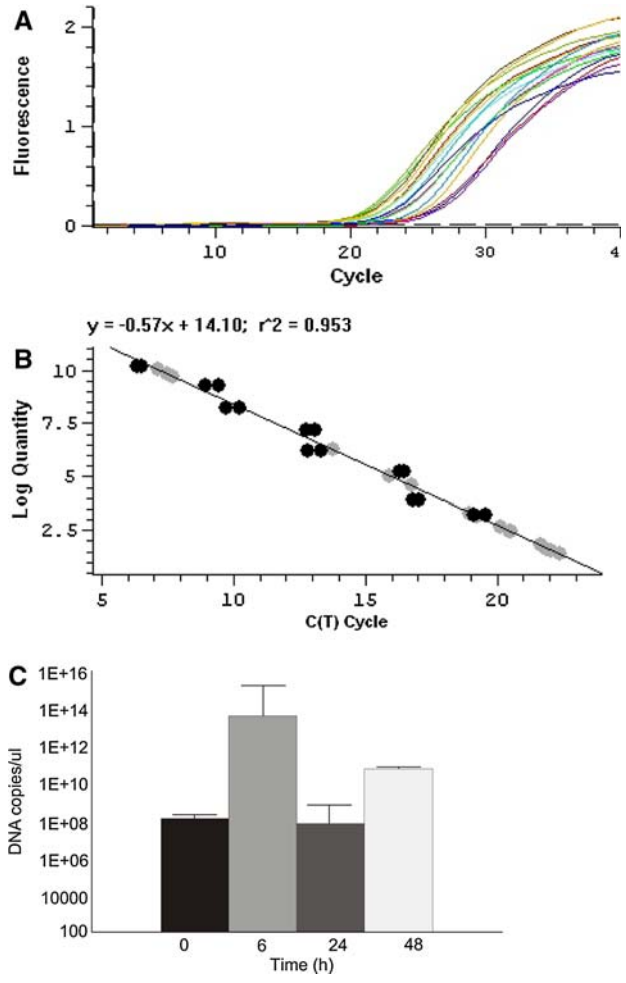

Fig. 2 Results of real-time PCR examination of caspase-1 expression in the rat jejunum. **a** Data graph, **b** standards graph, **c** histogram of gene expression over time, where data shown is group mean + SEM ($n = 6$)

been shown to be up-regulated at both the protein and mRNA levels following various cytotoxic treatments in intestinal cells. The transcriptional control of caspase-1 in the intestine is less well defined. In a previous study, irinotecan increased caspase-1 mRNA expression in myeloid leukaemia cells [40] and it was suggested that this would enhance apoptotic cell death. Another chemotherapy agent, cisplatin, has also been shown to increase caspase-1 mRNA expression in malignant glioma cells [24]. Apoptosis induced by cisplatin and also by forced caspase-1 overexpression is suppressed by the caspase-1 inhibitor Ac-YVAD-CMK, suggesting its requirement for apoptotic cell death in this model. Further to this, caspase-1 mRNA expression is often down-regulated in colon cancer [18], an environment of decreased apoptosis, indicating a disruption to the normal apoptotic pathway. Gene knockout studies of caspase-1 have also shown effective inhibition of apoptosis in response to various treatments. Caspase-1 appears to play a major role in damage-induced apoptosis in many settings.

In addition to its role in apoptosis, caspase-1 is responsible for the proteolysis and maturation of pro-inflammatory cytokines, namely interleukin-1β (IL-1β) and IL-18 [11, 26]. Activation of the TNF receptor through an increase in circulating TNF also induces caspase-1 activation as part of the MAPK signalling pathway, an important stress kinase pathway [25]. Therefore, the up-regulation of caspase-1 in the rat jejunum by irinotecan may induce an inflammatory response. However, we have found that irinotecan treatment caused minimal inflammation with lamina propria oedema and degenerate polymorphonuclear cells within crypts, but with no increases in inflammatory cells within the lamina [13]. Thus overt inflammation was not present and suggests that the alternative mechanism of caspase-1-induced apoptosis is more likely.

We also found that a range of other genes were altered by irinotecan treatment and their regulation provides information about the action of the drug on normal intestinal cells. For example, DPD is known to be closely associated with the toxicity of the chemotherapy agent 5-fluorouracil (5-FU). DPD is the first and rate-limiting enzyme in the catabolism of 5-FU [20]. DPD deficiency leads to impaired breakdown of 5-FU and therefore increases cytotoxicity, with patients with low levels of DPD at an increased risk of high-grade mucositis development [10, 19]. Up-regulation of this enzyme in response to irinotecan treatment could reduce toxic CPT-11 or SN-38, the active metabolite of irinotecan. Another enzyme, already characterised for its role in irinotecan-induced toxicity, is uridine diphosphate (UDP)-glucuronyl-transferase (UGT1A1) [3], which was up-regulated in this study. UGT1A1 is involved in the glucuronidation of SN-38 and is important for detoxification of SN-38. UGT1A1 glucuronidates and transforms SN-38 into the inactive form SN38 glucuronide (SN 38G), which is excreted in the bile by the small intestine. In cases of low UGT1A1 activity, the accumulation of high levels of SN-38 can cause severe diarrhoea and leucopaenia [37].

Genes involved in the immune response were highly represented both in the up- and down-regulated list, suggesting that irinotecan does induce an early, if somewhat mild, inflammatory response in the small intestine despite the immunosuppressive nature of chemotherapy treatment. The polymeric immunoglobulin receptor (pIgR), which mediates the transport of IgA across intestinal epithelial cells and provides immune protection at a number of levels has been shown to increase in inflammation. During the acute inflamma-

tory phase, there is up-regulation of TNF with subsequent activation of NFκB, which has been shown to interact and transcriptionally up-regulate the *pIgR* gene [7]. The transferrin receptor has also shown to be up-regulated in response to inflammation [4, 8, 39] and here may also indicate changes in iron homeostasis because of irinotecan treatment. On the down-regulated side, we first have CD59, which is also known as protectin. CD-59 is expressed on gut epithelium and is the main defence of cells against complement. It has previously been shown to be decreased in regions of inflammation [38] and it has been postulated that loss of CD59 could be a marker of injured cells waiting for clearance by the complement system [49]. The complement component 1 was down-regulated in this trial however, indicating that inflammatory mediators are not responsible for driving caspase activation in response to irinotecan at this time point.

The down-regulation of protective genes appears to be a major strategy by irinotecan to induce tissue injury. For example, multiple members of the tissue inhibitor of metalloproteinase (TIMP) family along with serine protease inhibitor and cystatin (a cystine protease inhibitor) were decreased in the treated group. The requirement for a balance in expression between cell destructive matrix metalloproteinases (MMP) and their inhibitors, TIMPs in tissue homeostasis has been shown clearly by a previous experiment in which during 5-FU-induced oral mucositis, there was an increase in MMP-2 and MMP-9 with concurrent decreases in TIMP-1 and TIMP-2 in damaged hamster cheek pouches [33]. Further to this, stabilisation of TIMP expression by the anti-inflammatory agent RG1503 prevented mucositis in the model. Second, metallothionein acts in the cell to bind zinc, which has numerous protective and healing roles in the intestine [48]. Metallothionein has also been shown to sequester free radicals during inflammatory states and thus contribute to cellular protection [34]. As such, decreases in the gene will be detrimental to overall intestinal integrity after irinotecan.

This study has shown that irinotecan has wide ranging effects on gene expression in the rat intestine and that a combination of apoptotic and inflammatory changes along with changes in cell cycling and metabolism all contribute to the damage seen following treatment. Importantly this study has identified MAP kinase signalling as being involved with irinotecan-induced intestinal damage and confirms previous findings with radiation-induced oral mucosal damage which also implicated this pathway [43]. This is a novel finding, strengthening the hypothesis that mucositis has the same pathogenesis in response to both types of anti-cancer treatment. The common caspase cascade-utilising pathway of chemotherapy- and radiotherapy-induced damage may be a useful target to prevent apoptosis following treatment and is applicable to all cancer patients.

Acknowledgments The authors wish to acknowledge Dr Ashley Connelly and the Adelaide Microarray Facility for assistance with this project, and Pfizer for the supply of the irinotecan. J. Bowen was supported by a Dawes Research Fellowship (Royal Adelaide Hospital) for the duration of this study.

References

1. Alimonti A, Gelibter A, Pavese I, Satta F, Cognetti F, Ferretti G et al (2004) New approaches to prevent intestinal toxicity of irinotecan-based regimens. Cancer Treat Rev 30(6):555–562
2. Altmann SW, Davis HR Jr, Zhu LJ, Yao X, Hoos LM, Tetzloff G et al (2004) Niemann-Pick C1 Like 1 protein is critical for intestinal cholesterol absorption. Science 303(5661): 1201–1204
3. Ando Y, Hasegawa Y (2005) Clinical pharmacogenetics of irinotecan (CPT-11). Drug Metab Rev 37(3):565–574
4. Barisani D, Parafioriti A, Bardella MT, Zoller H, Conte D, Armiraglio E et al (2004) Adaptive changes of duodenal iron transport proteins in celiac disease. Physiol Genomics 17(3):316–325
5. Boushey RP, Yusta B, Drucker DJ (2001) Glucagon-like peptide (GLP)-2 reduces chemotherapy-associated mortality and enhances cell survival in cells expressing a transfected GLP-2 receptor. Cancer Res 61(2):687–693
6. Bowen JM, Gibson RJ, Keefe DM, Cummins AG (2005) Cytotoxic chemotherapy upregulate pro-apoptotic Bax and Bak in the small intestine of rats and humans. Pathology 37(1):56–62
7. Bruno ME, Kaetzel CS (2005) Long-term exposure of the HT-29 human intestinal epithelial cell line to TNF causes sustained up-regulation of the polymeric Ig receptor and proinflammatory genes through transcriptional and post-transcriptional mechanisms. J Immunol 174(11):7278–7284
8. Cairo G, Pietrangelo A (1995) Nitric oxide-mediated activation of iron-regulatory protein controls hepatic iron metabolism during acute inflammation. Eur J Biochem 232(2):358–363
9. Cao S, Black JD, Troutt AB, Rustum YM (1998) Interleukin 15 offers selective protection from irinotecan-induced intestinal toxicity in a preclinical animal model. Cancer Res 58(15): 3270–3274
10. Chu QS, Hammond LA, Schwartz G, Ochoa L, Rha SY, Denis L et al (2004) Phase I and pharmacokinetic study of the oral fluoropyrimidine S-1 on a once-daily-for-28-day schedule in patients with advanced malignancies. Clin Cancer Res 10(15):4913–4921
11. Creagh EM, Conroy H, Martin SJ (2003) Caspase activation pathways in apoptosis and immunity. Immunol Rev 193:10–21
12. Gibson RJ, Bowen JM, Inglis MR, Cummins AG, Keefe DM (2003) Irinotecan causes severe small intestinal damage, as well as colonic damage, in the rat with implanted breast cancer. J Gastroenterol Hepatol 18(9):1095–1100
13. Gibson RJ, Bowen JM, Keefe DM (2005) Palifermin reduces diarrhea and increases survival following irinotecan treatment in tumor-bearing DA rats. Int J Cancer 116(3):464–470

14. Gibson RJ, Keefe DM, Clarke JM, Regester GO, Thompson FM, Goland GJ et al (2002) The effect of keratinocyte growth factor on tumour growth and small intestinal mucositis after chemotherapy in the rat with breast cancer. Cancer Chemother Pharmacol 50(1):53–58
15. Gibson RJ, Keefe DM, Thompson FM, Clarke JM, Goland GJ, Cummins AG (2002) Effect of interleukin-11 on ameliorating intestinal damage after methotrexate treatment of breast cancer in rats. Digestive Dis Sci 47(12): 2751–2757
16. Grutter MG (2000) Caspases: key players in programmed cell death. Curr Opin Struct Biol 10(6):649–655
17. Ikuno N, Soda H, Watanabe M, Oka M (1995) Irinotecan (CPT-11) and characteristic mucosal changes in the mouse ileum and cecum. J Natl Cancer Inst 87(24):1876–1883
18. Jarry A, Vallette G, Cassagnau E, Moreau A, Bou-Hanna C, Lemarre P et al (1999) Interleukin 1 and interleukin 1 beta converting enzyme (caspase 1) expression in the human colonic epithelial barrier. Caspase 1 downregulation in colon cancer. Gut 45(2):246–251
19. Johnson MR, Hageboutros A, Wang K, High L, Smith JB, Diasio RB (1999) Life-threatening toxicity in a dihydropyrimidine dehydrogenase-deficient patient after treatment with topical 5-fluorouracil. Clin Cancer Res 5(8):2006–2011
20. Katona C, Kralovanszky J, Rosta A, Pandi E, Fonyad G, Toth K, et al. (1998) Putative role of dihydropyrimidine dehydrogenase in the toxic side effect of 5-fluorouracil in colorectal cancer patients. Oncology 55(5):468–474
21. Keefe DM (2004) Gastrointestinal mucositis: a new biological model. Support Care Cancer 12(1):6–9
22. Keefe DM, Brealey J, Goland GJ, Cummins AG (2000) Chemotherapy for cancer causes apoptosis that precedes hypoplasia in crypts of the small intestine in humans. Gut 47(5):632–637
23. Keefe DM, Gibson RJ, Hauer-Jensen M (2004) Gastrointestinal mucositis. Semin Oncol Nurs 20(1):38–47
24. Kondo S, Barna BP, Morimura T, Takeuchi J, Yuan J, Akbasak A et al (1995) Interleukin-1 beta-converting enzyme mediates cisplatin-induced apoptosis in malignant glioma cells. Cancer Res 55(24):6166–6171
25. Lamkanfi M, Kalai M, Saelens X, Declercq W, Vandenabeele P (2004) Caspase-1 activates nuclear factor of the kappa-enhancer in B cells independently of its enzymatic activity. J Biol Chem 279(23):24785–24793
26. Launay S, Hermine O, Fontenay M, Kroemer G, Solary E, Garrido C (2005) Vital functions for lethal caspases. Oncogene 24(33):5137–5148
27. Lavrik IN, Golks A, Krammer PH (2005) Caspases: pharmacological manipulation of cell death. J Clin Invest 115(10):2665–2672
28. Lonnstedt I, Britton T (2005) Hierarchical Bayes models for cDNA microarray gene expression. Biostatistics 6(2):279–291
29. Lönnstedt I, Speed TP (2002) Replicated microarray data. Statistica Sinica 12:31–46
30. Marshman E, Ottewell PD, Potten CS, Watson AJ (2001) Caspase activation during spontaneous and radiation-induced apoptosis in the murine intestine. J Pathol 195(3):285–292
31. Martinon F, Tschopp J (2004) Inflammatory caspases: linking an intracellular innate immune system to autoinflammatory diseases. Cell 117(5):561–574
32. Morelli D, Menard S, Colnaghi MI, Balsari A (1996) Oral administration of anti-doxorubicin monoclonal antibody prevents chemotherapy-induced gastrointestinal toxicity in mice. Cancer Res 56(9):2082–2085
33. Morvan FO, Baroukh B, Ledoux D, Caruelle JP, Barritault D, Godeau G et al (2004) An engineered biopolymer prevents mucositis induced by 5-fluorouracil in hamsters. Am J Pathol 164(2):739–746
34. Mulder TP, van der Sluys Veer A, Verspaget HW, Griffioen G, Pena AS, Janssens AR et al (1994) Effect of oral zinc supplementation on metallothionein and superoxide dismutase concentrations in patients with inflammatory bowel disease. J Gastroenterol Hepatol 9(5):472–477
35. Philchenkov A (2004) Caspases: potential targets for regulating cell death. J Cell Mol Med 8(4):432–444
36. Pico J, Avila-Garavito A, Naccache P (1998) Mucositis: its occurrence, consequences and treatment in the oncology setting. Oncologist 3:446–451
37. Russo A, Corsale S, Cammareri P, Agnese V, Cascio S, Di Fede G et al (2005) Pharmacogenomics in colorectal carcinomas: future perspectives in personalized therapy. J Cell Physiol 204(3):742–749
38. Scheinin T, Bohling T, Halme L, Kontiainen S, Bjorge L, Meri S (1999) Decreased expression of protectin (CD59) in gut epithelium in ulcerative colitis and Crohn's disease. Hum Pathol 30(12):1427–1430
39. Schreiber S, MacDermott RP, Raedler A, Pinnau R, Bertovich MJ, Nash GS (1991) Increased activation of isolated intestinal lamina propria mononuclear cells in inflammatory bowel disease. Gastroenterology 101(4):1020–1030
40. Shibata Y, Takiguchi H, Tamura K, Yamanaka K, Tezuka M, Abiko Y (1996) Stimulation of interleukin-1 beta-converting enzyme activity during growth inhibition by CPT-11 in the human myeloid leukemia cell line K562. Biochem Mol Med 57(1):25–30
41. Smyth GK (2004) Linear models and empirical Bayes methods for assessing differential expression in microarray experiments. Statist Appl Genet Mol Biol 3(1):2004
42. Sonis ST (2004) A biological approach to mucositis. J Support Oncol 2(1):21–32; discussion 35–36
43. Sonis ST (2004) The pathobiology of mucositis. Nat Rev Cancer 4(4):277–284
44. Sonis ST (2004) Pathobiology of mucositis. Semin Oncol Nurs 20(1):11–15
45. Sonis ST, Elting LS, Keefe D, Peterson DE, Schubert M, Hauer-Jensen M et al (2004) Perspectives on cancer therapy-induced mucosal injury: pathogenesis, measurement, epidemiology, and consequences for patients. Cancer 100(9 suppl):1995–2025
46. Sonis ST, Scherer J, Phelan S, Lucey CA, Barron JE, O'Donnell KE et al (2002) The gene expression sequence of radiated mucosa in an animal mucositis model. Cell Prolif 35(suppl 1):93–102
47. Takasuna K, Hagiwara T, Hirohashi M, Kato M, Nomura M, Nagai E et al (1996) Involvement of beta-glucuronidase in intestinal microflora in the intestinal toxicity of the antitumor camptothecin derivative irinotecan hydrochloride (CPT-11) in rats. Cancer Res 56(16):3752–3757
48. Tran CD, Howarth GS, Coyle P, Philcox JC, Rofe AM, Butler RN (2003) Dietary supplementation with zinc and a growth factor extract derived from bovine cheese whey improves methotrexate-damaged rat intestine. Am J Clin Nutr 77(5):1296–1303
49. Vakeva A, Laurila P, Meri S (1992) Loss of expression of protectin (CD59) is associated with complement membrane attack complex deposition in myocardial infarction. Lab Invest 67(5):608–616
50. Yang YH, Buckley MJ, Speed TP (2001) Analysis of cDNA microarray images. Brief Bioinform 2(4):341–349
51. Yu J, Shannon WD, Watson MA, McLeod HL (2005) Gene expression profiling of the irinotecan pathway in colorectal cancer. Clin Cancer Res 11(5):2053–2062